

**PSFC/JA-11-35**

**H-mode power threshold reduction in a slot divertor  
configuration on the Alcator C-Mod tokamak**

Y.Ma, J.W.Hughes, A.E.Hubbard, B.LaBombard, J.Terry

December, 2011

**Plasma Science and Fusion Center  
Massachusetts Institute of Technology  
Cambridge MA 02139 USA**

This work was supported by the U.S. Department of Energy, Grant No. DE-FC02-99ER54512. Reproduction, translation, publication, use and disposal, in whole or in part, by or for the United States government is permitted.

# H-mode power threshold reduction in a slot divertor configuration on the Alcator C-Mod tokamak

Y.Ma, J.W.Hughes, A.E.Hubbard, B.LaBombard, J.Terry  
*Massachusetts Institute of Technology, Plasma Science and Fusion center  
175 Albany Street, Cambridge, MA 02139 USA*

H-mode power thresholds ( $P_{th}$ ) are examined in Alcator C-Mod lower single null plasmas with standard vertical-plate and slot-type divertor configuration ( $B_T=5.4\text{T}$ ,  $I_p=0.9\text{MA}$ ,  $q_{95}\sim 4.0$ , and  $\langle n_e \rangle = 1.3\text{--}1.6 \times 10^{20} \text{m}^{-3}$ ). The required power to access H-mod is found to be significantly reduced when the plasma is operated with slot divertor. The lowest  $P_{th}$  achieved is  $\sim 0.6\text{MW}$ , about 1/3 of the normal level and 40% of the multi-machine scaling law prediction.  $P_{th}$  does not correlate with plasma shaping parameters (X-point locations, elongation, etc), but shows a strong inverse correlation with outer divertor leg length (poloidal distance between X-point and outer strike point) and/or divertor connection length. Despite the large differences in  $P_{th}$ , the edge electron temperature ( $T_e$ ) and density ( $n_e$ ) profiles prior to L-H transition are not strongly affected by divertor configuration. Values of  $T_{e,95}$  (i.e.,  $T_e$  at 95% normalized poloidal flux surface) at L-H transition are similar for the two divertor configurations.

## 1. Introduction

In order to develop high performance operational scenarios for future tokamak fusion devices, a reliable prediction of the threshold power ( $P_{th}$ ) needed to access the H-mode confinement regime is required. At the present time, multi-machine scaling laws are used to estimate  $P_{th}$ , the most widely used one being [1],  $P_{scaling} [MW] = 0.049 \bar{n}_e [10^{20} \text{m}^{-3}]^{0.72} B_T [T]^{0.8} S [m^2]^{0.94}$ , which is valid for standard magnetic configuration with favorable ion  $\nabla B$  drift (i.e., pointing towards X-point), and for density above the “device-dependent low density limit” for H-mode access ([2]–[6]). This scaling law indicates that the three dominant dependencies are plasma density ( $\bar{n}_e$ ), strength of toroidal magnetic field ( $B_T$ ), and the plasma surface area ( $S$ ). However, ongoing experiments from many devices discovered that other variables may also strongly affect  $P_{th}$ . One example, found in JET [7], DIII-D [8], and MAST [9], is the so called “X-point height”, which is the vertical distance between X-point and the divertor plate. Motivated by these observations, we have undertaken experiments in Alcator C-Mod to explore the influence from the variation of X-point position and divertor geometry variables. We also observed that  $P_{th}$  can be strongly affected by the position of the X-point in relation to divertor surfaces. However, the most important parameter identified in our experiment appears to be the outer divertor leg length (poloidal distance between X-point and outer strike point) and/or the divertor connection length. Remarkably low values of  $P_{th}$  are found in slot-divertor configuration where the outer divertor leg length increases by  $\sim 50\text{--}100\%$  from normal values, while  $P_{th}$  decreases by a factor of  $\sim 2$  or even more.

## 2. Experimental setup

The experiment was performed within a single day of C-Mod plasma operation. The toroidal magnetic field ( $B_T$ ) and plasma current ( $I_p$ ) were fixed at  $B_T = 5.4\text{--}5.5\text{T}$  and  $I_p = 0.9\text{MA}$ , thus  $q_{95} \sim 4.0$ . All discharges were deuterium plasmas, created in lower single null magnetic configuration with ion  $\nabla B$  drift in the favorable direction for H-mode access. The line averaged plasma density  $\bar{n}_e$  at L-H transition was controlled between  $1.3 \times 10^{20} \text{m}^{-3}$  and  $1.6 \times 10^{20} \text{m}^{-3}$  for these plasmas; the Greenwald fraction  $\bar{n}_e / n_G$  was approximately  $0.25\text{--}0.28$ , correspondingly, the divertor was in the high-recycling regime [10]. An important reason for choosing this target density range is to minimize the influence of plasma density on  $P_{th}$ . Previous experiments identified a local minimum in  $P_{th}$  was versus  $\bar{n}_e$  for  $\bar{n}_e$  in the range  $\bar{n}_e \sim 1.2\text{--}1.7 \times 10^{20} \text{m}^{-3}$  [11]. All L-H transitions in this experiment were achieved with the addition of ICRF auxiliary heating power. The antenna frequency was tuned at  $\sim 80\text{MHz}$  to facilitate

on-axis fundamental hydrogen minority heating. Minority ion density concentration relative to main ion ( $n_H/n_D$ ) was maintained approximately constant and close to 5% throughout the experiment. Under these conditions, efficient single pass absorption of ICRF power is maintained [12]. ICRF power was injected during the plasma current flat-top of each discharge; the magnitudes were increased either in small steps or in a slow continuous ramp-up pattern.

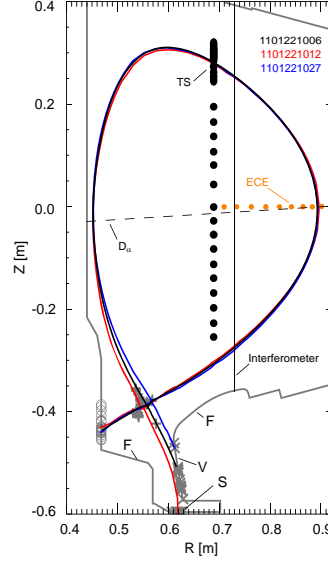


Fig.1. C-Mod poloidal cross-section showing locations of X-point (+), outer (X) and inner (open circles) separatrix strike points investigated. Examples of separatrix contours for vertical plate (blue) and slot (red) divertor operation are shown. Separatrix contour for a standard C-Mod magnetic geometry is also shown (black). C-Mod facilitates three different divertor configurations: flat-plate, vertical, and slot divertor, achieved by placing outer separatrix strike point on the divertor plate(s) labeled “F”, “V”, and “S”, respectively. Measurement locations of Thomson scattering (solid black circle) and ECE (orange), and the viewing cord of midplane  $D_\alpha$  emission (dashed line) are also displayed.

Variation of the lower null position results in three effectively different divertor configurations [10]. Based on where the outer separatrix strike point (OSP) is placed on the divertor plate, these configurations are called flat-plate (F), vertical-plate (V), and slot (S) divertor as illustrated in Fig.1. Standard C-Mod plasma operation is realized with vertical-plate divertor; contour plot of the separatrix for typical C-Mod magnetic geometry is shown in Fig.1

During the experiment, the X-point location was repositioned after each plasma discharge. As a result, plasma shaping parameters at L-H transition were subject to some variation:  $\kappa \sim 1.5-1.7$ ,  $\delta_{lower} \sim 0.45-0.65$ ,  $\delta_{upper} \sim 0.27-0.45$ , inner and outer gap  $\sim 1$ cm. Compared to shaping parameters, the variation in OSP locations was dramatic: it was scanned from the top of the vertical plate to the horizontal floor of the slot. Consequently, the outer leg length, which is defined as the poloidal distance between X-point and OSP, was significantly varied from  $\sim 10$  cm to  $\sim 25$  cm. Locations of X-point, inner and outer strike point just before L-H transition from these discharges are shown in Fig. 1 over a C-Mod poloidal cross section.

Some key C-Mod diagnostics were involved in this experiment. The Thomson scattering (TS) system operated with two Nd:YAG lasers each at 30Hz and pulsed alternatively is used as the main diagnostic for electron temperature ( $T_e$ ) and density ( $n_e$ ) along a vertical chord through the magnetic axis. The spatial resolution of TS measured profiles, when mapped to midplane using EFIT, is  $1\sim 2$ cm in plasma core and  $1\sim 2$ mm in the plasma edge. Electron cyclotron emission (ECE) polychromators provide sub *ms* midplane electron temperature measurements with reduced spatial resolution of  $\sim 1$ cm across the midplane minor radius. The line averaged plasma density  $\bar{n}_e$  is recorded by a multi-chord two-color CW interferometer system. A photodiode array was employed to provide a single-chord

midplane  $H_\alpha$  and  $D_\alpha$  emission measurement. Measurement locations for each diagnostics described above are illustrated on Fig.1.

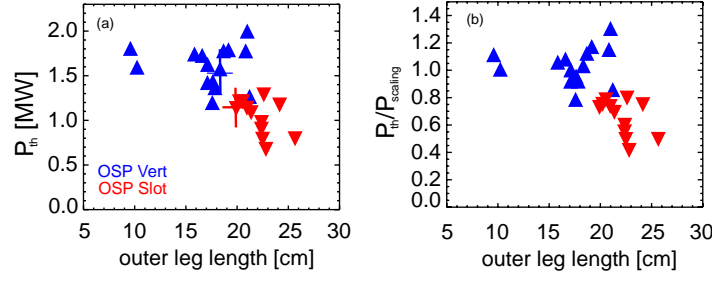


Fig.2. L-H power thresholds, (a)  $P_{th}$  and (b)  $P_{th}/P_{scaling}$ , as a function of the poloidal distance between X-point and outer strike point (outer leg length, OLL).  $P_{th}$  is systematically lower when the plasma is operated with a slot divertor (red) compared to a vertical plate divertor (blue).

### 3. Reduction of H-mode threshold power

The H-mode threshold power  $P_{th}$  is defined as [1]  $P_{loss} = P_{tot} - dW_{MHD}/dt = P_{OH} + P_{RF} - dW_{MHD}/dt$ , assessed at the L-H transition time. Here,  $P_{RF}$  is the net ICRF power launched by the antennas, assumed to be 100% absorbed by plasma. The ohmic power  $P_{OH}$  and stored plasma energy  $W_{MHD}$  are evaluated using the equilibrium magnetic reconstruction code EFIT [13].

The most remarkable result from this experiment is that  $P_{th}$  is strongly reduced with slot divertor operation. This is demonstrated in Fig. 2:  $P_{th}$  and  $P_{th}/P_{scaling}$  with slot divertor (red) are significantly reduced relative to vertical-plate divertor geometry (blue). The minimum  $P_{th}$  obtained is  $\sim 0.6$  MW, which is approximately 1/3 of the normal value ( $P_{th} = 1.5 \sim 1.8$  MW in standard C-Mod magnetic geometry), and only  $\sim 40\%$  of the multi-machine scaling law prediction. This result is significant and perhaps promising for H-mode access at reduced power.

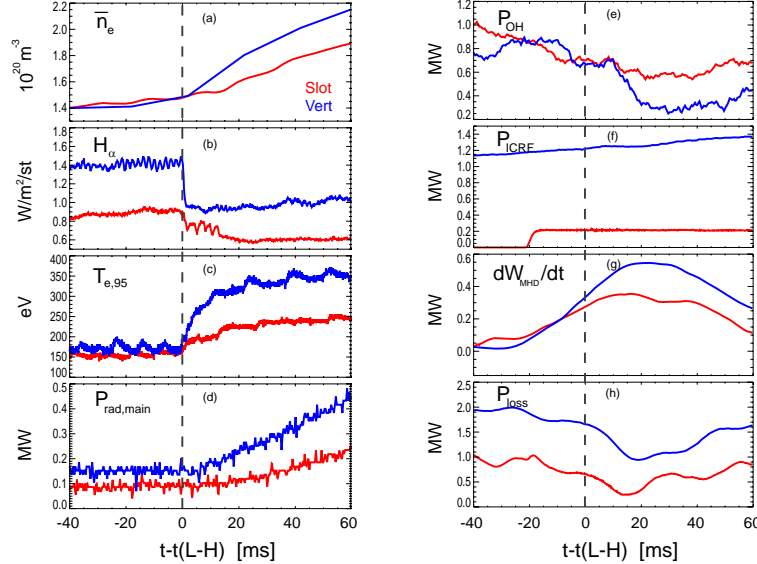


Fig.3. Comparison of L-H transition time evolution for two discharges with vertical plate (blue) and slot (red) divertor operation: (a) line averaged density (b) midplane  $H_\alpha$  emission (c)  $T_e(\psi=0.95)$  from ECE (d) radiated power from bulk plasma  $P_{rad,main}$  (e) ohmic power  $P_{OH}$  (f) ICRF power  $P_{RF}$  (g)  $dW_{MHD}/dt$  (h)  $P_{loss} = P_{OH} + P_{RF} - dW_{MHD}/dt$ . The time base has been shifted so that the origin is aligned with the L-H transition time.

The reduction of  $P_{th}$  is clearly seen by the reduction in auxiliary heating power needed ( $P_{RF}$ ) to obtain an H-mode. Figure 3 shows a comparison of time histories of L-H transition indicators (left) and each individual component of  $P_{loss}$  (right) from two typical plasma discharges with different divertor configurations. Note that the time base for each discharge has been shifted so that the origin is aligned with the L-H transition times. We notice that for the two cases,  $P_{OH}$  and  $dW_{MHD}/dt$  at L-H transition are nearly the same; however, the difference in  $P_{RF}$  is remarkable: with slot divertor, H-mode can be induced with a tiny amount of  $P_{RF}$  at  $\sim 0.2\text{MW}$ , whereas about  $1.0\text{MW}$  is required for vertical plate divertor operation.

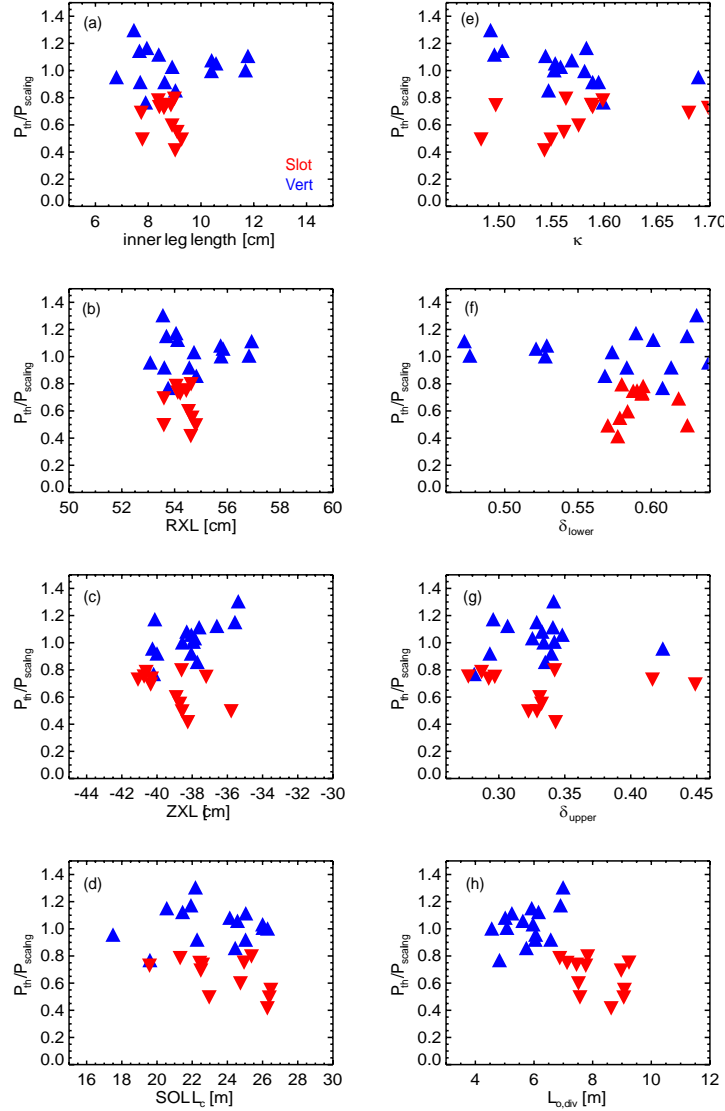


Fig.4. Normalized H-mode threshold power ( $P_{th}/P_{scaling}$ ) displayed as a function of geometry parameters: (a) inner leg length, (b) major radius of X-point ( $RXL$ ), (c) vertical position of X-point to midplane ( $ZXL$ ), (d) SOL connection length  $L_c$ , (e) elongation  $\kappa$ , (f) lower triangularity  $\delta_{lower}$ , (g) upper triangularity  $\delta_{upper}$ , (h) connection length from outboard midplane to outer divertor.  $L_{o,div}$  shows the clearest correlation with  $P_{th}/P_{scaling}$ .

In Fig. 4, normalized L-H threshold powers,  $P_{th}/P_{scaling}$ , are displayed against a number of other potentially relevant shaping parameters, including inner leg length,  $RXL$  (major radius of X-point),  $ZXL$  (vertical position of X-point relative to the midplane),  $\kappa$ ,  $\delta_{lower}$ ,  $\delta_{upper}$ ,  $L_c$  (total scrape-off layer connection length), and  $L_{o,div}$  (connection length from outboard midplane to OSP). Only  $L_{o,div}$ , which

is essentially covariant with OLL in this experiment, shows a correlation with threshold power. The correlation coefficients  $r$ , defined as

$$r = \frac{\sum_i (x_i - \bar{x})(y_i - \bar{y})}{\sqrt{\sum_i (x_i - \bar{x})^2 \sum_i (y_i - \bar{y})^2}}$$

between  $P_{th}/P_{scaling}$  and the above parameters (also OLL) reveals equally strong inverse correlation of  $P_{th}/P_{scaling}$  with  $L_{o,div}$  ( $r=-0.519$ ) and OLL ( $r=-0.482$ ), while the correlation of  $P_{th}/P_{scaling}$  with other examined parameters are weak ( $-0.25 < r < 0.15$ ).

#### 4. Local edge conditions

Figure 5 shows the radial profiles (midplane-mapped using EFIT reconstruction) of electron temperature ( $T_e$ ), density ( $n_e$ ), and the normalized inverse scale length  $a_0/L_T = (a_0/T_e)(dT_e/dr)$ ,  $a_0/L_n = (a_0/n_e)(dn_e/dr)$  preceding L-H transitions in the edge and near scrape-off layer (SOL) region of plasma. These profiles are obtained from the last two laser pulses prior to each L-H transition, and radially shifted to obtain  $T_e$  values at the separatrix ( $r/a=1.0$ ) that are consistent with a two-point SOL-divertor power balance model [14]. The required radial shifts are less than 5 mm, and typically 1.5~3mm. The time interval between the earlier pulse and L-H transition time is typically 20~30 ms, which is comparable to or shorter than a typical energy and particle confinement time. Under the assumption that plasma equilibria do not evolve substantially within a confinement time, these profiles are expected to be close to those at the L-H transition. Surprisingly, despite the large discrepancy in  $P_{th}$ , we find little difference in the  $T_e$  and  $n_e$  profiles between slot and vertical plate divertor configurations.

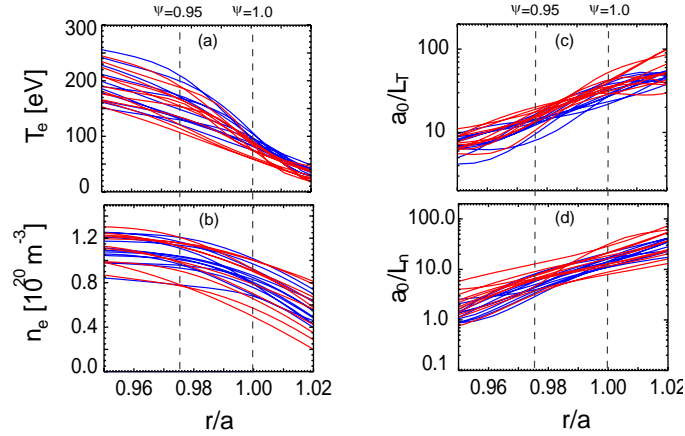


Fig.5. Radial profiles of (a) electron temperature  $T_e$ , (b) electron density  $n_e$ , and their scale lengths (c)  $a_0/L_T = (a_0/T_e)dT_e/dr$ , (d)  $a_0/L_n = (a_0/n_e)dn_e/dr$  across the separatrix, taken within 20~30 ms before L-H transitions. These profiles are obtained by fitting the EFIT-mapped Thomson scattering  $T_e$  and  $n_e$  measurements from the last two laser pulses prior to L-H transition and shifting them in radius to match the expected values of  $T_e$  at separatrix ( $r/a=1.0$ ,  $\psi=1.0$ ), based on a two-point SOL-divertor power balance model. Dash lines represent the approximate radial locations for  $\psi=0.95$  ( $r/a \sim 0.975$ ) surface and the last closed flux surface ( $\psi=1.0$ ) from EFIT magnetic reconstruction.

The high time-resolution ECE radiometers facilitate instantaneous electron temperature measurements on the outer midplane. The ECE measurements of  $T_{e,95}$  (i.e.,  $T_e$  at 95% normalized poloidal flux surface  $\psi=0.95$ ) at L-H transition are shown in Fig. 6 as a function of  $P_{th}$ . The uncertainties in the separatrix radial locations could give rise to estimated errors of 30-50 eV in ECE measured  $T_{e,95}$ . Despite the fact that the slot divertor tends to have lower  $P_{th}$  values,  $T_{e,95}$  values at the time of L-H transition are comparable to those with vertical plate divertor. While  $T_{e,95}$  scatters between 100eV and 200eV, no clear dependence on  $P_{loss}$  is observed within estimated experimental uncertainties. This temperature range is also consistent with that obtained from earlier C-Mod studies [15]. We also note with ICRH, the edge  $T_e$  can be transiently higher due to sawtooth heat pulses, as seen in Figure 3.c.

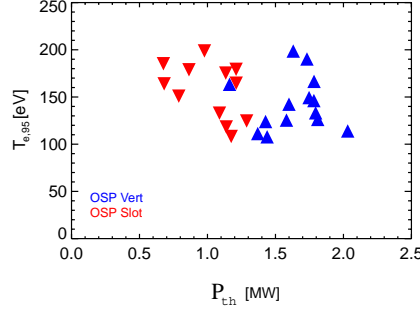


Fig.6. ECE measurements of  $T_{e,95}$  ( $T_e$  at  $r \sim a_0 - 8mm$ ) at L-H transition as a function of  $P_{th}$ . Changing the divertor configuration does not appear to affect  $T_{e,95}$  at the L-H transition.

## 5. Discussion and conclusion

In summary, our divertor configuration experiments have uncovered a strong correlation in  $P_{th}$  with OLL or  $L_{o,div}$ , such that  $P_{th}$  decreases with increasing OLL or  $L_{o,div}$ , while keeping the multi-machine scaling law parameters fixed (i.e.,  $\bar{n}_e$ ,  $B_T$ , and  $S$ ). It should be noted that this trend is *opposite* to that observed in JET [7], DIII-D [8] and MAST [9], if their results are instead interpreted in the context of OLL (the X-point height and OLL are covariant in these experiments). It is not clear whether this phenomenon is due to some unique features of C-Mod tokamak, e.g. high toroidal field, divertor shape, etc. Although  $T_{e,95}$  at L-H transition appears to be not affected by divertor configuration, the ion temperature, plasma rotation, and radial electric field for L-H transition, which are not well characterized in this experiment, might be strongly altered when the divertor configuration is changed. This is a topic for further investigation.

## Reference

- [1] Martin Y.R., et al., *Journal of Physics; Conference Series* **123** (2008) 012033
- [2] S.J. Fielding et al. *PPCF* **38** (1996) 1091.
- [3] J.A. Snipes et al, *PPCF* **38** (1996) 1127
- [4] T. Carlstrom and R.J. Groebner, *Phys. Plasmas* **3** (1996) 1867
- [5] Y. Andrew et al *PPCF* **48** (2006) 479
- [6] F. Ryter et al. *Nucl. Fusion* **49** (2009) 062003
- [7] Andrew Y, et al 2004 *Plasma Phys. Control. Fusion* **46** A87
- [8] P. Gohil et al. *Nucl. Fusion* **51** (2011) 103020.
- [9] H. Meyer et al. *Nucl. Fusion* **51** (2011) 113011
- [10] Lipschultz B, et al 2007 *Fusion Science and Technology* 51
- [11] Ma Y, et al, *Scaling of H-mode threshold power and L-H edge conditions with favorable ion grad-B drift in Alcator C-Mod tokamak*, submitted to *Nucl Fusion*
- [12] Bonoli P, *Fusion Science and Techonlogy*, **51** pp.401
- [13] Lao L.L., et al, *Nucl. Fusion* **30** (1990) 1035
- [14] B.Labombard, private communication.
- [15] Hubbard A.E, et al, *Plasma Phys. Control. Fusion* **40** (1998)